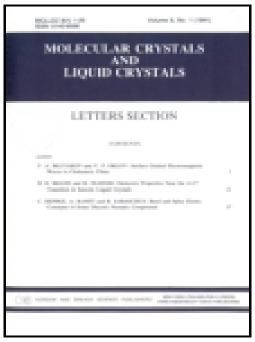

Taylor & Francis
Taylor & Francis Group

Molecular Crystals and Liquid Crystals

ISSN: 1542-1406 (Print) 1563-5287 (Online) Journal homepage: http://www.tandfonline.com/loi/gmcl20

High-Efficiency Dicyanobenzene-Based Organic Light-Emitting Diodes Exhibiting Thermally Activated Delayed Fluorescence

Geon Hyeong Lee, Dong Yuel Kwon & Young Sik Kim

To cite this article: Geon Hyeong Lee, Dong Yuel Kwon & Young Sik Kim (2015) High-Efficiency Dicyanobenzene-Based Organic Light-Emitting Diodes Exhibiting Thermally Activated Delayed Fluorescence, Molecular Crystals and Liquid Crystals, 621:1, 1-7, DOI: 10.1080/15421406.2015.1095450

To link to this article: http://dx.doi.org/10.1080/15421406.2015.1095450

Mol. Cryst. Liq. Cryst., Vol. 621: pp. 1–7, 2015
Copyright © Taylor & Francis Group, LLC
ISSN: 1542-1406 print/1563-5287 online
DOI: 10.1080/15421406.2015.1095450

Taylor & Francis
Taylor & Francis Group

High-Efficiency Dicyanobenzene-Based Organic Light-Emitting Diodes Exhibiting Thermally Activated Delayed Fluorescence

GEON HYEONG LEE,[1] DONG YUEL KWON,[1]
AND YOUNG SIK KIM[1,2,*]

[1]Department of Information Display, Hongik University, Seoul, Korea
[2]Department of Science, Hongik University, Seoul, Korea

We have designed novel thermally activated delayed fluorescence (TADF) materials, 2DMACPN and 2DMACTPN, with 9,9-dimethyl-9,10-dihydroacridine (DMAC) as an electron donor and dicyanobenzene as an electron acceptor. We obtain the zero-zero transition energies of the first excited singlet (S_1) and first triplet excited (T_1) states of TADF materials by performing density functional theory (DFT) and time-dependent density functional theory (TD-DFT) calculations on the ground state using a dependence on charge transfer amounts for the optimal Hartree-Fock percentage in the exchange-correlation of TD-DFT. The calculated ΔE_{ST} values of 2DMACPN (0.019 eV) and 2DMACTPN (0.023 eV) were smaller than those of 2CzPN (0.363eV) and 2CzTPN (0.178eV) because of the large dihedral angles between the plane of DMAC and the connected phenyl rings of PN and TPN. We show that 2DMACPN would have the highest TADF efficiency among the four compounds because it has the largest dihedral angle, which creates a small spatial overlap between the HOMO and the LUMO, and consequently the smallest ΔE_{ST}.

Keywords OLED; Thermally activated delayed fluorescence (TADF); DFT; TD-DFT

1. Introduction

Organic light-emitting diodes (OLEDs) have been widely investigated because of their low-voltage operation, wide-viewing angle, high contrast, mechanical flexibility, and potential applications in flat-panel displays.[1] In fluorescent OLEDs, only 25% of the excitons can emit light because carrier recombination produces singlet and triplet excitons in a 1:3 ratio through spin statics.[2] Phosphorescent OLEDs based on noble heavy-metal phosphors can produce both singlet and triplet excitons by enhanced spin-orbit coupling (SOC) and can achieve nearly 100% internal quantum efficiency, which corresponds to an external electroluminescent (EL) quantum efficiency of close to 20% without enhanced out-coupling techniques.[3,4] However, phosphorescent materials containing noble metals such as Ir(III),

---

[*]Address correspondence to Young Sik Kim, Department of Information Display, Hongik University, Seoul 121-791, Korea. E-mail: youngkim@hongik.ac.kr

Color versions of one or more of the figures in the article can be found online at www.tandfonline.com/gmcl.

Pt(II), and Os(II) are rather expensive and unsustainable. Therefore, a novel method for achieving high EL efficiency is required.

A newly introduced triplet harvesting method that uses thermally activated up-conversion of triplet into singlet states has recently been shown to provide thermally activated delayed fluorescence (TADF) with high photoluminescence efficiency.[5] Charge-transfer (CT) systems confirmed TADF with a small gap between the lowest singlet (S_1) and triplet (T_1) excited states. The S_1 level is considerably higher in energy than the T_1 level by $0.5 \sim 1.0$ eV because of the electron exchange energy between these levels. Promotion of TADF requires a small energy gap (ΔE_{ST}) between the S_1 state and T_1 state because the rate of $T_1 \rightarrow S_1$ reverse intersystem crossing (RISC) is inversely proportional to the exponential of ΔE_{ST}.[6] Because ΔE_{ST} largely depends on the exchange interaction between electrons in molecular orbitals, implying electronic excitation, the spatial overlap between molecular orbitals must be controlled. Thus, the molecular design of TADF emitters involves a careful choice of suitable donor and acceptor units.

One important factor in designing molecules with a small ΔE_{ST} is to have a negligible spatial overlap between the highest occupied molecular orbital (HOMO) and the lowest unoccupied molecular orbital (LUMO).[7] The strategies for obtaining a negligible spatial overlap between the HOMO and LUMO are: (1) to have a large dihedral angle between the plane of the donor and the connected phenyl rings of the acceptor, and (2) to increase the spatial distance between the donor and acceptor constituents with a π-conjugation linker.

Previously reported blue TADF emitters showed some strongly localized states with $^3\pi\pi^*$ or $^3n\pi^*$ character that were lower in energy than the ^{3}CT state.[8] This indicated that ΔE_{ST} can be minimized by adjusting the energy levels of the ^{1}CT state and the lowest locally excited triplet state (^{3}LE). Increasing the twist angle between donor and acceptor units limits their electronic interaction, which stabilizes the CT state and increases the energy of ^{3}LE state,[9] although this is insufficient to ensure that the ^{3}CT state is lower than ^{3}LE. The Adachi group previously reported a computational prediction for singlet and triplet transition energies of charge transfer compounds using the optimal Hartree-Fock (HF) exchange method to predict the ^{1}CT, ^{3}CT, and ^{3}LE levels of molecules.[8]

In this study, we designed two novel thermally activated delayed fluorescence (TADF) molecules, 4,5-bis(9,9-dimethyl-9,10-dihydroacridinyl) phthalonitrile (2DMACPN) and 2,5-bis(9,9-dimethyl-9,10-dihydroacridinyl)-1,4-dicyanobenzene (2DMACTPN), where dicyanobenzene serves as the electron acceptor and 9,9-dimethyl-9,10-dihydroacridine(DMAC) is the electron donor (Fig. 1). We compared these TADF molecules to 4,5-bis(carbazole-9-yl) phthalonitrile (2CzPN) and 2,5-bis(carbazole-9-yl)) -1,4-dicyanobenzene (2CzTPN), which use carbazole as the electron donor. In addition, we evaluated the substitution positions of dicyanobenzene in terms of their electronic and optical properties in order to enhance the TADF efficiency.

2. Computational Methods

We investigated the factors responsible for the absorption energy and the electron population of molecular orbitals by performing density functional theory (DFT) and time-dependent density functional theory (TD-DFT) calculations on the ground state, using a dependence on the amount of charge transfer (CT) from donor to acceptor for the optimal HF percentage in the TD-DFT exchange-correlation. The geometries in the gas phase were optimized by the DFT method using the B3LYP exchange-correlation function with the 6-31G* basis set in the Gaussian 09 program package.[10] The possible isomers of the dyes were also calculated by DFT.

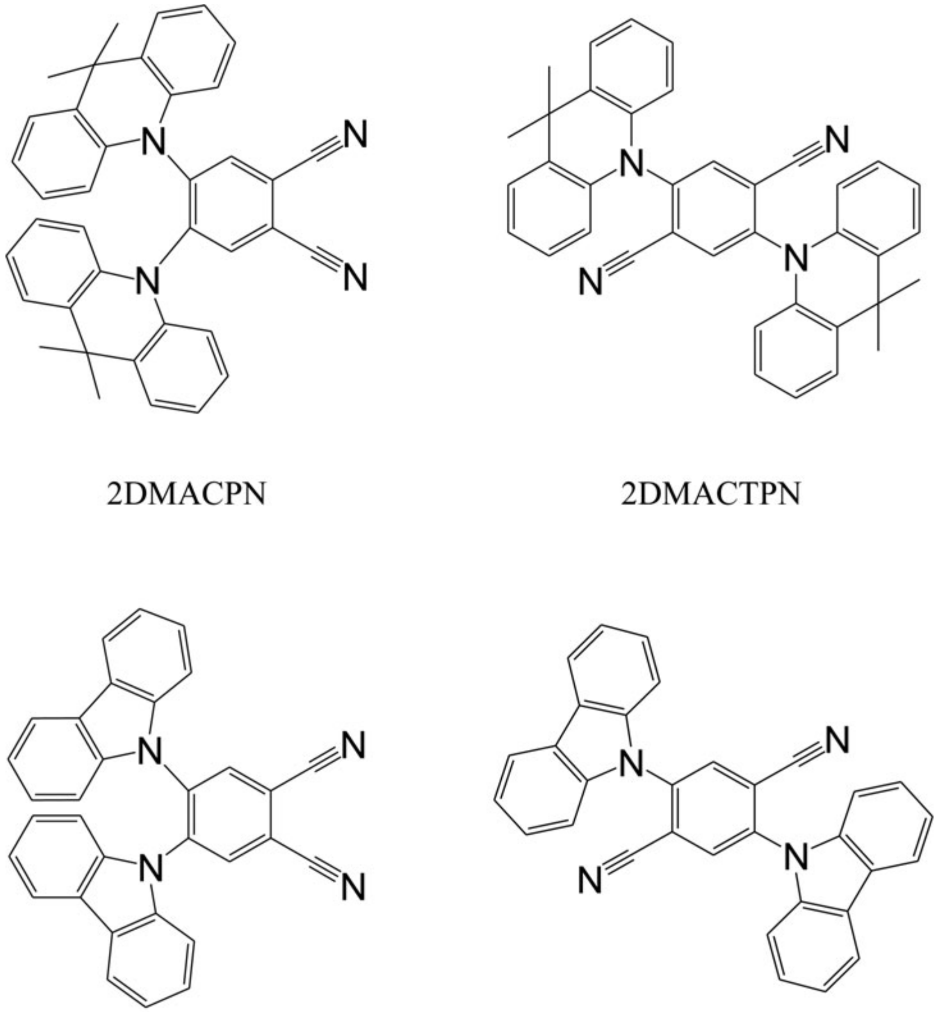

2DMACPN 2DMACTPN

2CzPN 2CzTPN

Figure 1. Chemical structures of 2DMACPN, 2DMACTPN, 2CzPN, and 2CzTPN.

The conformation presented here was the lowest energy conformation, which is the optimal molecular structure of the dyes in the gas phase. The electronic populations of the highest occupied molecular orbital (HOMO) and the lowest unoccupied molecular orbital (LUMO) were calculated to show the position of electron populations according to the calculated molecular orbital energy diagram. Vertical absorption energies [E_{VA}] were calculated by TD-DFT with the BLYP, MPW1B95, BMK, M062X, and M06HF functionals using 6-31G* basis sets. We determined an optimal HF% (OHF) by using the Multiwfn program to analyze the orbital composition for obtaining a CT amount (q) from the donor to the acceptor; the optimal HF% is proportional to the CT amount with a relation of OHF = 42q. We calculated $E_{VA}(S_1,OHF)$, $E_{VE}(S_1,OHF)$, and $E_{0\text{-}0}(^1CT)$ using a

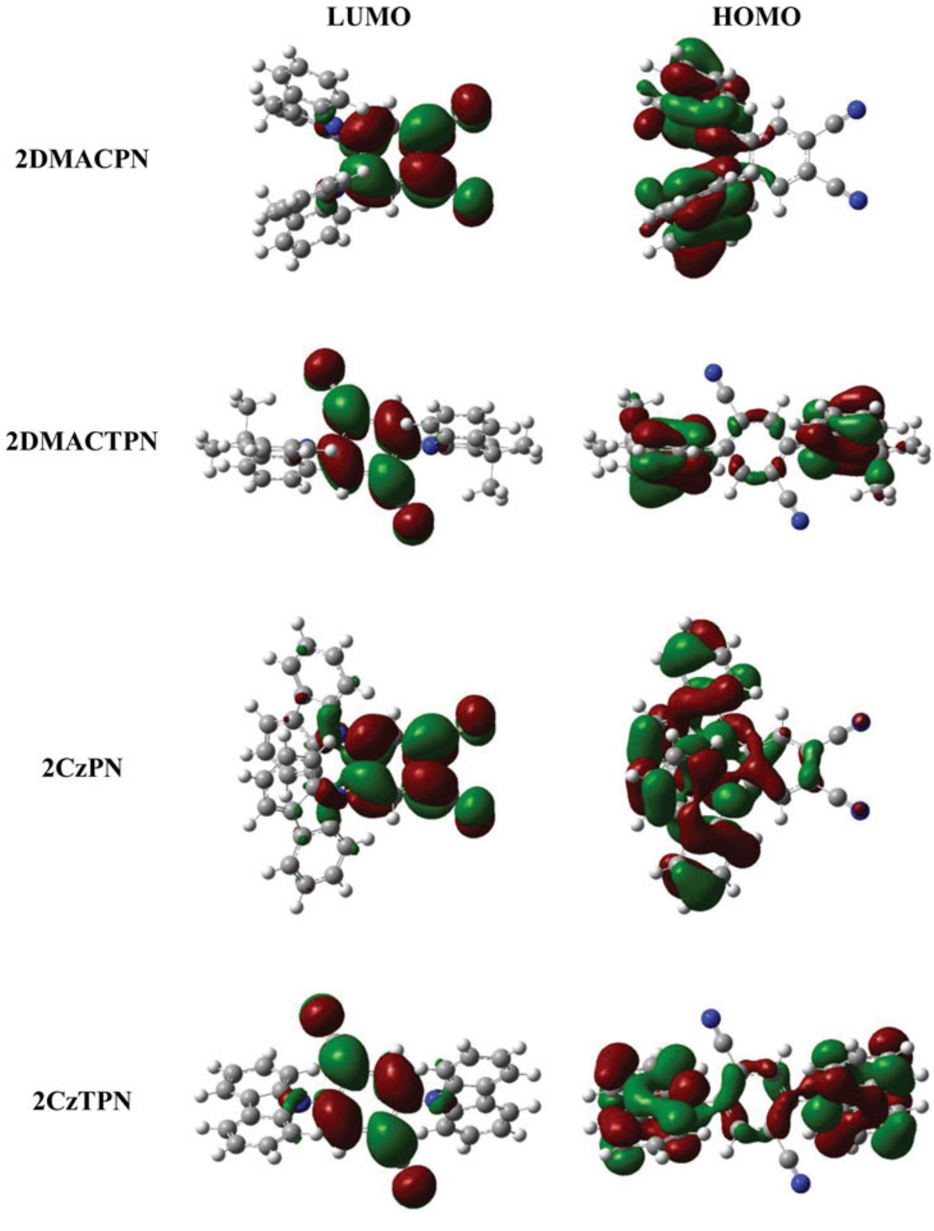

Figure 2. HOMO and LUMO distribution of 2DMACPN, 2DMACTPN, 2CzPN, and 2CzTPN.

common gap of 0.24 eV between $E_{VA}(S_1,OHF)$ and $E_{0\text{-}0}(^1CT)$. We set as $E_{VE}(S_1.OHF) = E_{VA}(S_1,OHF) + 0.48$ eV. The value for $E_{VA}(T_1)$ corresponding to the ^3CT or ^3LE transitions and calculations for $E_{0\text{–}0}(^3CT)$ and $E_{0\text{–}0}(^3LE)$ were obtained by the proven methods of Adachi et al.[8]

3. Results And Discussion

The chemical structures of the materials investigated in the present study are shown in Fig. 1. The reference materials of 2CzPN and 2CzTPN containing a carbazole moiety as a donor unit and a dicyanobenzene as an acceptor unit exhibited a TADF emission.[11,12] A series of dicyanobenzene derivatives were designed in which the donor unit was changed from carbazole to DMAC to enhance the TADF efficiency.

The HOMO and the LUMO for these materials, calculated with the DFT method using the optimized ground-state molecular geometry, are shown in Fig. 2. The HOMO distribution is largely localized on the DMAC moiety, while the LUMO is localized on the dicyanobenzene moiety, resulting in a small overlap between the HOMO and the LUMO. These novel materials with DMAC as an electron donor have similar HOMO/LUMO characteristic properties but with much smaller overlap than seen with previous materials that used carbazole as an electron donor. This is because the dihedral angles between the plane of DMAC and its connected phenyl rings of PN and TPN were very large values of 82.1° and 79.9°, respectively, resulting in small overlap between the HOMO and the LUMO (compared with the dihedral angles of 51.9° and 56.3° for 2CzPN and 2CzTPN, respectively). Because ΔE_{ST} largely depends on the exchange interaction between electrons in molecular orbitals, a smaller spatial overlap between the HOMO and the LUMO leads to a smaller ΔE_{ST}. A small ΔE_{ST} between the S_1 state and T_1 state increases the rate of $T_1 \rightarrow S_1$ upconversion and harvests formally spin-forbidden T_1 excitons.

Table 1 shows the calculated ΔE_{ST} of each material using a dependence on charge transfer amounts for the optimal HF percentage in the exchange-correlation of DFT. The experimental ΔE_{ST} of 2CzPN (0.31 eV)[11] and 2CzTPN (0.08 eV)[12] and the calculated ΔE_{ST} of 2CzPN (0.363 eV) and 2CzTPN (0.178 eV) show only slight differences. Therefore, the computational method can be used for comparing the change in relative ΔE_{ST}. The calculated ΔE_{ST} values of 2DMACPN (0.019 eV) and 2DMACTPN (0.023 eV) were smaller than those of 2CzPN (0.363eV) and 2CzTPN (0.178eV) because of the large dihedral angles between the planes of the donor and acceptor units. The calculated ΔE_{ST} values indicate that 2DMACPN would show the highest TADF efficiency.

We examined the effect of the substitution position of dicyanobenzene by comparing the ΔE_{ST} values of 2CzPN (0.363eV), 2CzTPN (0.178eV), 2DMACPN (0.019 eV), and 2DMACTPN (0.023 eV). The ΔE_{ST} value was smaller for 2CzTPN than for 2CzPN;

Table 1. Calculated data using various exchange-correlation functionals and 6-31G* basis set based on B3LYP optimized geometries

parameter	2CzPN	2CzTPN	2DMACPN	2DMACTPN
CT amount (q)	0.7547	0.8012	0.8305	0.8721
Optimal HF%	32%	34%	35%	37%
$E_{VA}(S_1, OHF)$ (eV)	3.169	2.859	2.548	2.607
$E_{VE}(S_1)$ (eV)	2.689	2.379	2.068	2.127
$E_{0\text{-}0}(^1CT)$ (eV)	2.929	2.619	2.308	2.367
$E_{0\text{-}0}(^3CT)$ (eV)	2.665	2.442	2.289	2.344
$E_{0\text{-}0}(^3LE)$ (eV)	2.566	2.485	2.566	2.580
ΔE_{ST} (eV)	0.363	0.178	0.019	0.023
dihedral angle (°)	51.9	56.3	82.1	79.9

however, the ΔE_{ST} value was larger for 2DMACTPN than for 2DMACPN. This probably reflects a larger steric hindrance between the donor unit and the cyano moiety than between the donor and donor units. Thus, the steric hindrance is larger for 2CzTPN than for 2CzPN, which increases the dihedral angle between the carbazole and acceptor unit. However, the dihedral angle between the DMAC and the acceptor group is about 90°, so the larger steric hindrance of 2DMACTPN results in a smaller dihedral angle between the DMAC and the acceptor group. The largest dihedral angle between the plane of donor and the phenyl ring of acceptor unit is obtained with 2DMACPN. This leads to a small spatial overlap between the HOMO and the LUMO, and consequently to the smallest ΔE_{ST} among the four compounds.

4. Conclusion

We designed two novel TADF molecules, 2DMACPN and 2DMACTPN, and compared them to 2CzPN and 2CzTPN in terms of the electronic and optical properties in order to enhance the TADF efficiency. An important factor in designing these molecules with a small ΔE_{ST} is to have a small spatial overlap between the HOMO and the LUMO, with a large dihedral angle between the plane of the donor and its connected phenyl rings of acceptor. The calculated ΔE_{ST} values in 2DMACPN (0.019 eV) and 2DMACTPN (0.023 eV) were smaller than that in 2CzPN (0.363eV) and 2CzTPN (0.178eV) because of the large dihedral angles between the plane of DMAC and its connected phenyl rings of PN and TPN. The largest dihedral angle of 2DMACPN leads to the smallest spatial overlap between the HOMO and the LUMO, and consequently to the smallest ΔE_{ST} among the four compounds. Thus, 2DMACPN would show the highest TADF efficiency among the four compounds.

Acknowledgment

This research was supported by the Basic Science Research Program through the National Research Foundation of Korea (NRF) funded by the Ministry of Education, Science and Technology (2010-0021668).

References

[1] Tang, C. W. and Vanslyke, S. A. (1987). *Appl. Phys. Lett.*, *51*, 913; Adachi, C., Tsutsui, T. and Saito, S. (1989). *J. Appl. Phys.,* 55, 813; Baldo, M. A., Lamansky, S., Burrows, P. E., Tompson, M. E. and Forrest, S. R. (1999). *Appl. Phys. Lett.,* 75, 4; Baldo, M. A., Thompson, M. E. and Forrest, S. R. (2000). *Nature*, 403, 750.

[2] Huang, C. W., Peng, K. Y., Liu, C. Y., Jen, T. H., Yang, N. J. and Chen, S. A. (2008). *Adv. Mater.*, *20*, 3709; Zhang, Y., Lai, S. L., Tong, Q. X., Lo, M. F., Ng, T. W., Chan, M. Y., Wen, Z. C., He, J., Jeff, K. S., Tang, X. L., Liu, W. M., Ko, C. C., Wang, P. F. and Lee, C. S. (2012). *Chem. Mater.,* 24, 61.

[3] Baldo, M. A., O'Brien, D. F., You, Y., Shoustikov, A., Sibley, S., Thompson, M. E. and Forrest, S. R. (1998). *Nature. 395*, 151; Adachi, C., Baldo, M. A., Thompson, M. E. and Forrest, S. R. (2001). *J. Appl. Phys.* 90, 5048.

[4] Ham, H. W., Jung, K. Y. and Kim, Y. S. (2010). *Thin Solid Film. 518*, 6199; Park, S. W. Ham, H. W. and Kim, Y. S. (2012). *J. Nanosci. Nanotechnol.* 12, 3369.

[5] Kondakov, D. Y., Pawlik, T. D., Hatwar, T. K. and Spindler, J. P. (2009). *J. Appl. Phys. 106*, 124510; Endo, A., Sato, K., Yoshimura, K., Kai, T., Kawada, A., Miyazak, H. and Adachi, C.

(2011). *Appl. Phys. Lett.* 98, 083302; Goushi, K., Yoshida, K., Sato, K. and Adachi, C. (2012). *Nat. photonics.* 6, 253.

[6] Berberan-Santos, M. N. and Garcia, J. M. M. (1996). *J. Am. Chem. Soc. 118*, 9391.

[7] Lee, J., Shizu, K., Tanaka, H., Nomura, H., Yasuda, T., and Adachi, C. (2013). *J. Mater. Chem. 1*, 4599.

[8] Huang, S., Zhang, Q., Shiota, Y., Nakagawa, T., Kuwabara, K., Yoshizawa, K. and Adachi, C. (2013). *J. Chem. Theory Comput. 9*, 3872.

[9] Grabowski, Z. R., Rotkiewicz, K. and Rettig, W. (2003). *Chem. Rev. 103*, 3899–4031.

[10] Nasu, K., Nakagawa, T., Nomura, H., Lin, C., Cheng, C., Tseng, M., Yasuda, T. and Adachi, C. (2013). *Chem. Commun. 49*, 10385.

[11] Uoyama, H., Goushi, K., Shizu, K., Nomura, H. and Adachi, C. (2012). *Nature*. *492*, 234.

[12] Nishimoto, T., Yasuda, T., Lee, S. Y., Kondo, R. and Adachi, C. (2014) *Mater. Horiz. 1*, 264.